Detailed study of the astrophysical direct capture reaction ^{6}Li$(p, \gamma)^7$Be in a potential model approach

E. M. Tursunov [*]
Institute of Nuclear Physics, Academy of Sciences, 100214 Ulugbek, Tashkent, Uzbekistan and National University of Uzbekistan, 100174 Tashkent, Uzbekistan

S. A. Turakulov [†]
Institute of Nuclear Physics, Academy of Sciences, 100214 Ulugbek, Tashkent, Uzbekistan

K. I. Tursunmakhatov [‡]
Department of Physics, Gulistan State University, 120100 Gulistan, Uzbekistan

(Received 23 June 2023; accepted 9 November 2023; published 1 December 2023)

The astrophysical S factor and reaction rates of the direct capture process ^{6}Li$(p, \gamma)^7$Be are estimated within a two-body single-channel potential model approach. Nuclear potentials of the Gaussian form in the $^2P_{3/2}$ and $^2P_{1/2}$ waves are adjusted to reproduce the binding energies and the empirical values of the asymptotic normalization coefficients (ANC) for the ^{7}Be$(3/2^-)$ ground and ^{7}Be$(1/2^-)$ excited bound states, respectively. The parameters of the potential in the most important $^2S_{1/2}$ scattering channel were fitted to reproduce the empirical phase shifts from the literature and the low-energy astrophysical S factor of the LUNA Collaboration. The obtained results for the astrophysical S factor and the reaction rates are in very good agreement with available experimental data sets. The numerical estimates reproduce not only the absolute values, but also the energy dependence of the S factor and the temperature dependence of the reaction rates of the LUNA Collaboration. The estimated ^{7}Li/H primordial abundance ratio of $(4.67 \pm 0.04) \times 10^{-10}$ is consistent with recent big bang nucleosynthesis result of $(4.72 \pm 0.72) \times 10^{-10}$ after the Planck telescope observation.

DOI: 10.1103/PhysRevC.108.065801

I. INTRODUCTION

One of the main problems of nuclear astrophysics is an estimation of the present-day abundances of light elements [1,2]. The nuclear fusion processes with elements D (^{2}H), He, and Li are important in the big bang nucleosynthesis (BBN) models. However, a large part of present-day observed Li, Be, and B abundances are due to contribution of galactic cosmic-ray spallation processes [3].

It is established that less than half of the present-day ^{7}Li abundance in the solar system was produced during the BBN processes, and a large part was synthesized in stars [4]. At the same time, the present-day observed abundance of the ^{6}Li element is almost exclusively produced by cosmic-ray spallation processes of heavy nuclei [5]. The Spite plateau for the ^{7}Li primordial abundance, observed in old metal-poor halo stars, does not exist for the ^{6}Li element abundance [6,7].

The main source of the primordial ^{6}Li abundance in the BBN is believed to be a nuclear direct capture reaction $d(\alpha, \gamma)^6$Li, while the reactions ^{6}Li$(p, \alpha)^3$He and ^{6}Li$(p, \gamma)^7$Be are the most destructive channels [8,9]. A precise experimental results for the astrophysical S factor, reaction rates of the $d(\alpha, \gamma)^6$Li direct capture process, and the primordial abundance of the ^{6}Li element obtained by the LUNA collaboration at an underground facility [10,11] have been accurately described within the three-body model [12–16]. The theoretical model reproduced not only the absolute values but also the energy dependence of the astrophysical S factor and the temperature dependence of the reaction rates due to the correct treatment of the isospin mixing of about 0.5% in the final state. However, the primordial abundance of the ^{7}Li element is still a big challenge for all the nuclear astrophysics community around the world, since the astronomically observed abundance of this element is about three times less than the present-day BBN estimate [17].

Thus, the ^{6}Li/^{7}Li isotopic ratio is important for specifying the lithium production mechanisms, either via cosmic-ray spallation processes [18] or via stellar evolution [19], which modify the primordial ^{7}Li abundance. For this purpose, an accurate estimation of the astrophysical S factor of the ^{6}Li$(p, \gamma)^7$Be direct capture process is necessary. The cross section of this process influences many astrophysical scenarios, including BBN and stellar evolution.

From the experimental side, very few measurements of the astrophysical S factor of the above reaction have been performed. The experiments were usually carried out at higher energies due to the Coulomb barrier problem, so extrapolation

[*]tursune@inp.uz
[†]turakulov@inp.uz
[‡]tursunmahatovkahramon@gmail.com

to the low-energy region was necessary. In addition, the enhancement due to the electron screening effect must be taken into account [20]. The total uncertainty of the old data set from Ref. [21] is significant (∼15%), which makes an extrapolation to the low astrophysical-energy region quite difficult [22]. The most intriguing results have been reported in Ref. [23], which found a resonance at around 200 keV above the $p+{}^6$Li threshold with $J^\pi = 1/2^+$. However, that resonance was not seen in the data set for the $^3\mathrm{He}(\alpha,\gamma)^7\mathrm{Be}$ capture reaction [24]. Recent direct measurement of the $^6\mathrm{Li}(p,\gamma)^7\mathrm{Be}$ capture reaction by the LUNA Collaboration also does not support the existence of such a resonance [25].

The astrophysical $^6\mathrm{Li}(p,\gamma)^7\mathrm{Be}$ direct capture reaction has also been studied within various theoretical models, such as a potential model [26], a Gamow shell model [27], cluster models [7,28,29], and R-matrix fits [23,25,30]. The most successful description of the direct LUNA data has been reached within the asymptotic normalization coefficient (ANC) method [31]. The empirical values of the ANC for the $^6\mathrm{Li}+p\rightarrow{}^7\mathrm{Be}(3/2^-)$ and $^6\mathrm{Li}+p\rightarrow{}^7\mathrm{Be}(1/2^-)$ virtual transitions to the $^7\mathrm{Be}(3/2^-)$ ground and $^7\mathrm{Be}(1/2^-)$ excited bound states have been derived within the distorted-wave Born approximation (DWBA) from the analysis of the $^6\mathrm{Li}(^3\mathrm{He},d)^7\mathrm{Be}$ transfer reaction. Then on the base of deduced values of ANC the astrophysical S factor of the $^6\mathrm{Li}(p,\gamma)^7\mathrm{Be}$ direct capture reaction has been estimated at low energies [31]. As was proved in many cases, indirect techniques like the ANC method or the Trojan horse method can give important clues to the understanding of BBN (see, e.g., Ref. [32] for a review). However, the above work does not give a detailed information on the specific contribution of each entry channel to the capture process. In other words, contributions of the partial $E1$, $E2$, and $M1$ astrophysical S factors are not shown. On the other hand, the model does not probe the most important experimental data for the reaction rates of the LUNA Collaboration [25]. These studies are important for nuclear physics, since they allow one to find the most realistic $p+{}^6$Li potential parameters in each partial wave, both in the bound and scattering channels. Only a model which simultaneously reproduces the absolute values and the energy dependence of the astrophysical S factor and temperature dependence of the reaction rates can be considered as fully realistic.

Very recently, a detailed study of the above $^6\mathrm{Li}(p,\gamma)^7\mathrm{Be}$ direct capture process at astrophysical energies was performed within the potential model [28]. Various versions of the potential model have been suggested; however, none of them describe the astrophysical S factor and the reaction rates simultaneously. More precisely, the temperature dependence of the reaction rates of the LUNA Collaboration [25] was not reproduced within that model. Thus, the question of whether a potential model can simultaneously describe the astrophysical S factor and the reaction rates remains open.

The aim of present work is a detailed study of the $^6\mathrm{Li}(p,\gamma)^7\mathrm{Be}$ astrophysical direct capture reaction at low energies within a single-channel potential model where a channel spin is fixed by $S=1/2$. Potential cluster models can simultaneously describe the properties of bound states and scattering data [7,28]. They can reproduce phase shifts, binding energy, and an ANC. The importance of knowledge of the ANC in nuclear reactions and astrophysical processes and indirect ANC method was demonstrated in particular in Refs. [33–37]. A realistic potential model is constructed based on the results of the ANC study of Ref. [31] and the potential models of Refs. [28,38]. In other words, we demonstrate that the present potential model is able to reproduce the empirical ANC values for the $^7\mathrm{Be}(3/2^-)$ ground and $^7\mathrm{Be}(1/2^-)$ excited bound states deduced in Ref. [31] in addition to the experimental bound state energies. Construction of the potential model was performed within the standard technique [28,39].

We use the Gaussian nuclear potential [40–42] with the appropriate Coulomb part. This choice is equivalent to the choice of the Woods-Saxon nuclear potential. The two-parameter Gaussian potential together with the Coulomb term, leads to the correct asymptotic form of the wave function (Whittaker function) like the Woods-Saxon potential. This is why the two different Gaussian and Woods-Saxon potential models yield the same results for the low-energy nuclear astrophysics processes.

The potential parameters in the $^2S_{1/2}$ wave are adjusted to reproduce the empirical phase shifts [28,38] and the experimental astrophysical S factor of the LUNA Collaboration [25]. Then the ability of the model to reproduce the empirical reaction rates will be examined. Most interestingly, we present both absolute values and temperature dependence of the theoretical reaction rates in comparison with the results of the LUNA Collaboration.

The article is organized as follows: the theoretical model will be described in Sec. II. Section III is devoted to the analysis of numerical results. Conclusions are given in the last section.

II. THE BASIC FORMALISM OF THE TWO-BODY SINGLE-CHANNEL MODEL

A. Wave functions

According to the single-channel potential model [43–45], the initial and final states are defined by the factorized wave functions as

$$\Psi^J_{lS} = \frac{u^{(lSJ)}_E(r)}{r}\{Y_l(\hat{r})\otimes\chi_S(\xi)\}_{JM} \tag{1}$$

and

$$\Psi^{J_f}_{l_fS'} = \frac{u^{(l_fS'J_f)}(r)}{r}\{Y_{l_f}(\hat{r})\otimes\chi_{S'}(\xi)\}_{J_fM_f}, \tag{2}$$

respectively. The radial wave functions of the initial p-^{6}Li scattering states in the $^2S_{1/2}$, $^2P_{1/2}$, $^2P_{3/2}$, $^2D_{3/2}$, $^2D_{5/2}$, $^2F_{5/2}$, $^2F_{7/2}$ partial waves are described as solutions of the two-body Schrödinger equation

$$\left[-\frac{\hbar^2}{2\mu}\left(\frac{d^2}{dr^2}-\frac{l(l+1)}{r^2}\right)+V^{lSJ}(r)\right]u^{(lSJ)}_E(r) = Eu^{(lSJ)}_E(r), \tag{3}$$

where μ is the reduced mass of proton and ^{6}Li nucleus, $1/\mu = 1/m_1 + 1/m_2$, and $V^{lSJ}(r)$ is a two-body potential in the partial wave with quantum numbers l (orbital angular

momentum), S (spin), and J (total angular momentum). The wave function $u^{(l_f S' J_f)}(r)$ of the final $^2P_{3/2}$ ground and $^2P_{1/2}$ excited bound states are defined as solutions of the bound-state Schrödinger equation. The Schrödinger equation is solved using the high-accuracy Numerov algorithm. At large distances the asymptotics of the scattering wave function must satisfy the condition

$$u_E^{(lSJ)}(r) = \cos\delta_{lSJ}(E) F_l(\eta, kr) + \sin\delta_{lSJ}(E) G_l(\eta, kr), \tag{4}$$

where k is the wave number of the relative motion, η is the Zommerfeld parameter, F_l and G_l are regular and irregular Coulomb functions, respectively, and $\delta_{lSJ}(E)$ is the phase shift in the partial wave with quantum numbers (l, S, J).

The p-^{6}Li two-body nuclear potential is chosen in the Gaussian form as [7,28]

$$V^{lSJ}(r) = V_0 \exp(-\alpha_0 r^2) + V_c(r), \tag{5}$$

where the Coulomb part of the potential is based on the point-like charges [7,28].

B. Cross sections of the radiative-capture process

The cross section, the astrophysical S factor and the reaction rates are estimated using the accurate wave functions of the initial and final states. The total cross section of the radiative-capture process is expressed as a sum of cross sections for each final state [44,45]:

$$\sigma(E) = \sum_{J_f \lambda \Omega} \sigma_{J_f \lambda}(\Omega), \tag{6}$$

where $\Omega = E$ (electric transition) or M (magnetic transition), λ is a multiplicity of the transition, J_f is the total angular momentum of the final state. For a particular final state with total angular momentum J_f and multiplicity λ we have [44]

$$\sigma_{J_f\lambda}(\Omega) = \sum_J \frac{(2J_f+1)}{[S_1][S_2]} \frac{32\pi^2(\lambda+1)}{\hbar\lambda([\lambda]!!)^2} k_\gamma^{2\lambda+1} C^2(S) \times \sum_{lS} \frac{1}{k_i^2 v_i} \left| \left\langle \Psi^{J_f}_{l_f S'} \middle\| M^\Omega_\lambda \middle\| \Psi^J_{lS} \right\rangle \right|^2, \tag{7}$$

where l and l_f are the orbital momenta of the initial and final states, respectively; k_i and v_i are the wave number and speed of the p-^{6}Li relative motion in the entrance channel, respectively; S_1 and S_2 are spins of p and ^{6}Li; $S' = S = 1/2$ due to the use of the single-channel approximation. The $k_\gamma = E_\gamma/\hbar c$ is the wave number of the photon corresponding to energy $E_\gamma = E_{\rm th} + E$, where $E_{\rm th}$ is the threshold energy for the breakup reaction $\gamma + {}^7\mathrm{Be} \to {}^6\mathrm{Li} + p$. Constant $C^2(S)$ is a spectroscopic factor [22]. Within the potential approach where the bound and scattering properties (energies, phase shifts and scattering length) are reproduced, a value of the spectroscopic factor must be taken equal to 1 [46]. We also use shorthand notations $[S] = 2S+1$ and $[\lambda]!! = (2\lambda+1)!!$.

The reduced matrix elements are estimated between the initial Ψ^J_{lS} and final $\Psi^{J_f}_{l_f S'}$ states. The electric transition operator in the long-wavelength approximation reads as

$$M^{\rm E}_{\lambda\mu} = e \sum_{j=1}^{A} Z_j r'^{\lambda}_j Y_{\lambda\mu}(\hat{r}'_j), \tag{8}$$

where $\vec{r}'_j = \vec{r}_j - \vec{R}_{cm}$ is the position of the jth particle in the center-of-mass system.

The magnetic transition operator reads as [43,44]

$$M^{\rm M}_{1\mu} = \sqrt{\frac{3}{4\pi}} \sum_{j=1}^{A} \left[\mu_N \frac{Z_j}{A_j} \hat{l}_{j\mu} + 2\mu_j \hat{S}_{j\mu} \right] = \sqrt{\frac{3}{4\pi}} \left[\mu_N \left(\frac{A_2 Z_1}{A A_1} \frac{A_1 Z_2}{A A_2} \right) \hat{l}_{r\mu} + 2(\mu_1 \hat{S}_{1\mu} + \mu_2 \hat{S}_{2\mu}) \right], \tag{9}$$

where μ_N is the nuclear magneton, μ_j is the magnetic moment and $\hat{l}_{j\mu}$ ($\mu = -1, 0, +1$) is the projection of the orbital angular momentum of jth particle. The projection of the orbital angular momentum of the relative motion is denoted as $\hat{l}_{r\mu}$.

The explicit expressions for the reduced matrix elements of the electric and magnetic transition operators were given in Ref. [45]. In the above equations the spins of the particles are $S_1 = S_p = 1/2$ and $S_2 = S(^6\mathrm{Li}) = 1$, and magnetic momenta are taken as $\mu_p = 2.792847\mu_N$ and $\mu(^6\mathrm{Li}) = 0.822\mu_\mathrm{N}$ for the first and second particles, respectively.

Finally, the astrophysical S factor of the process is related to the cross section as [47]

$$S(E) = E\,\sigma(E)\exp(2\pi\eta). \tag{10}$$

TABLE I. Central V_M nuclear potential parameters for the p-^{6}Li interaction in different partial waves.

$^{2S+1}L_J$	V_0 (MeV)	α_0 (fm^{-2})	C_{LJ} (fm$^{-1/2}$)	$E^{^7\mathrm{Be}}_{FS}$ (MeV)
$^2S_{1/2}$	−52.0	0.297		−5.81
$^2P_{3/2}$	−76.6277	0.1750	2.191	
$^2P_{1/2}$	−74.8169	0.1731	2.070	
$^2D_{3/2}$	−86.0	0.094		−6.95
$^2D_{5/2}$	−88.0	0.094		−7.75
$^2F_{5/2}$	−111.6	0.10		
$^2F_{7/2}$	−44.34	0.05		

III. NUMERICAL RESULTS

A. Astrophysical S factor of the ^{6}Li$(p,\gamma)^7$Be reaction

The wave functions of initial and final states are found from the numerical solution of the Schrödinger equation in the entrance and exit channels with the $p - {}^6$Li central nuclear potentials of the Gaussian-form as defined in Eq.(5) with the corresponding point like Coulomb part. Hereafter the parameter values $\hbar^2/2u = 20.9008$ MeV fm^2, 1 u = 931.494 MeV, $m_p = 1.007\,276\,47$ u, $m(^6\mathrm{Li}) = 6.013\,477\,46$ u, and $\hbar c = 197.327$ MeV fm are used in numerical calculations.

The parameters of the Gaussian-form central potential model V_M are presented in Table I. The modified potential model V_M differs from the original model V_D of Ref. [28]

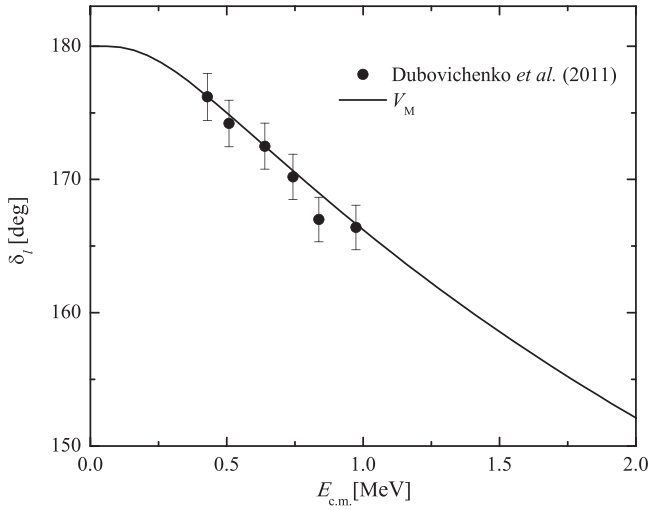

FIG. 1. Phase shift in the $^2S_{1/2}$ partial wave of the p-^{6}Li scattering state within the potential model V_M. The experimental phase shifts are taken from Ref. [38].

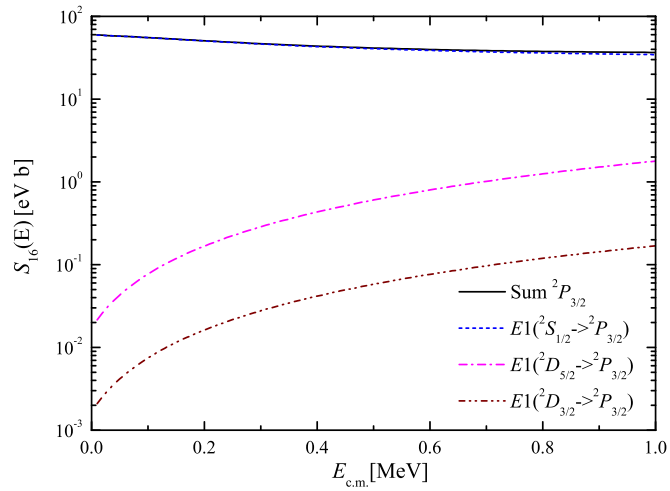

FIG. 2. The contributions of the $E1$ transition operator to the astrophysical S factor within the V_M potential model from different initial scattering states to the final ^{7}Be$(3/2^-)$ ground state.

in the $^2S_{1/2}$, $^2P_{1/2}$, $^2P_{3/2}$, $^2D_{3/2}$, and $^2D_{5/2}$ partial waves, while keeping the parameter values unchanged in the F- wave scattering channels.

The parameters of the modified V_M potential in the $^2P_{3/2}$ and $^2P_{1/2}$ partial waves are fitted to reproduce the experimental binding energies $E(3/2^-) = -5.6068$ MeV and $E(1/2^-) = -5.1767$ MeV and the empirical squared ANC values of 4.81 ± 0.38 fm^{-1} and 4.29 ± 0.27 fm^{-1} for the ^{7}Be$(3/2^-)$ ground and ^{7}Be$(1/2^-)$ excited bound states, respectively. The empirical values of ANC were obtained from the analysis of the experimental differential cross section of the proton-transfer reaction using a modified DWBA approach in Ref. [31].

The parameters of the modified V_M potential in the $^2S_{1/2}$ partial wave were fitted to reproduce the experimental phase shifts from Ref. [38] and the direct data of the LUNA Collaboration for the astrophysical S factor of the ^{6}Li$(p,\gamma)^7$Be capture reaction at low energies [25]. The calculated phase shifts for the p-^{6}Li scattering in the $^2S_{1/2}$ partial wave using modified V_M potential are presented in Fig. 1 in comparison with the experimental data from Ref. [38]. It shows that $E1$ transitions to the final P states play the main role in the synthesis reaction ^{6}Li$(p,\gamma)^7$Be. Therefore, the parameters of the V_M potential in the S wave can be adjusted to the experimental values of the astrophysical S factor of the LUNA Collaboration. In other words, from phase-equivalent potentials one can choose a model which can describe the experimental astrophysical S factor at low energies at a satisfactory level. The parameters of the model in the D-wave scattering channels are fitted to reproduce the astrophysical S factor at larger energies. As was noted in the Introduction, the main point here is a question of whether a potential model constructed in such a way will be able to reproduce simultaneously the both absolute values and temperature dependence of the reaction rates of the LUNA Collaboration without any additional parameters. This check is realistic in a sense that a correct model must describe the both absolute values and temperature dependence of the reaction rates, as was demonstrated in the study of the direct capture process $\alpha(d,\gamma)^6$Li [14,45].

Energies of the forbidden states in the $^2S_{1/2}$, $^2D_{3/2}$, $^2D_{5/2}$ partial waves of the p-^{6}Li relative motion are given in the last column of Table I. The Pauli forbidden states in all S and D waves correspond to the orbital configuration $[s^5p^2]$ [28].

The partial contributions of the $E1$ transition to the astrophysical S factor for the V_M potential from different initial scattering states to the final ^{7}Be$(3/2^-)$ ground state are shown in Fig. 2. As is seen from the figure, the dominant contribution corresponds to the $^2S_{1/2} \to {}^2P_{3/2}$ transition in the whole energy region up to 1 MeV.

Within the cluster model, the effect of antisymmetrization in the $p + {}^6$Li nuclear system is taken into account by means of the Pauli forbidden state in the S wave. In Fig. 3 we examine the effect of the antisymmetrization between the proton and the nucleons of ^{6}Li with the help of the supersymmetric transformation (SUSY) method of the initial S-wave potential [48]. The SUSY transformation of the initial S-wave

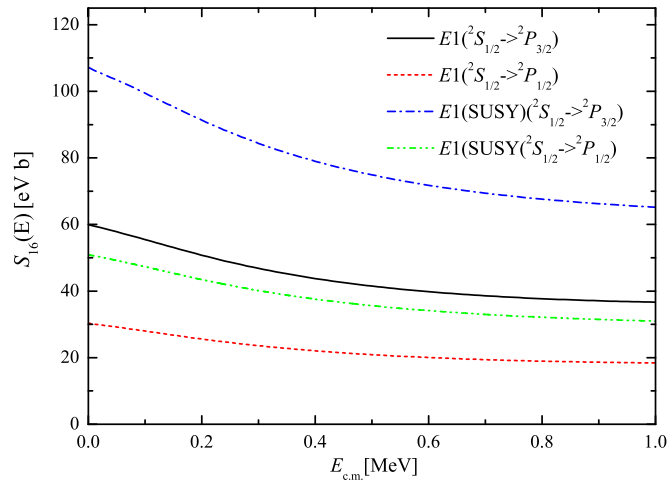

FIG. 3. Effect of the SUSY transformation of the S-wave potential on the $E1$ astrophysical S factor within the potential model V_M.

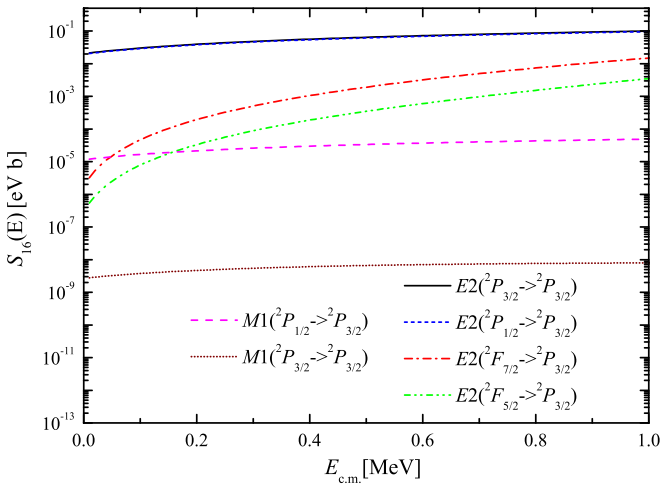

FIG. 4. The partial contributions of the $E2$ and $M1$ transition operators to the astrophysical S factor from different initial scattering states to the final ^{7}Be($3/2^-$) ground state within the V_M potential model.

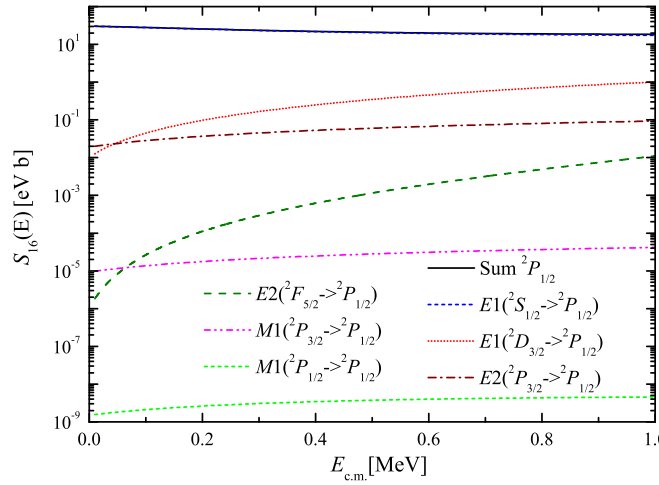

FIG. 5. Contributions of the $E1$, $E2$, and $M1$ transition operators to the astrophysical S factor from different initial scattering states to the final ^{7}Be($1/2^-$) excited bound state within the V_M potential model.

potential removes the forbidden bound state from the spectrum, while keeping unchanged the phase-shift description. Then we calculate the astrophysical $E1$ S factor with the SUSY transformed potential. In this way we remove the effect of antisymmetrization for the direct capture process. As can be seen from the figure, the result of the SUSY transformation of the original S-wave potential with a forbidden bound state is crucial for the astrophysical $E1$ S factor. After the SUSY transformation the astrophysical S factor increases approximately by factor 2 in the low energy region, thus the difference between the theoretical results and experimental data becomes noticeably large. The effect is connected with a nodal character of the S-wave scattering wave function in the internal region for the initial potential with a forbidden state. After the SUSY transformation, the node disappears, which increases the absolute value of the overlap integral of the initial scattering and final bound state wave functions. This means that the effect of antisymmetrization, which was taken into account by means of the forbidden states in the cluster model, is essential for the direct capture reaction ^{6}Li$(p,\gamma)^7$Be. And without the antisymmetrization effects (in other words, without the S-wave forbidden state), the experimental data for the astrophysical S factor and the reaction rates could not be described by the theoretical model.

The partial contributions of the $E2$ and $M1$ transitions to the astrophysical S factor from different initial scattering states to the final ^{7}Be($3/2^-$) ground state are shown in Fig. 4. As can be seen from the figure, these contributions are negligible compared to the contribution of the $E1$ transition in Fig. 2. They differ by more than three orders of magnitude.

In Fig. 5 the partial contributions of all $E1$, $E2$ and $M1$ transitions to the astrophysical S factor from different initial scattering states to the final ^{7}Be($1/2^-$) excited bound state are presented. As can be noted here, the most important contribution comes from the $E1$ transition $^2S_{1/2} \rightarrow {}^2P_{1/2}$.

Figure 6 shows a comparison of the contributions of the $E1$, $E2$, and $M1$ transition operators to the astrophysical S factor of the ^{6}Li$(p,\gamma)^7$Be synthesis process. As can be seen from the figure, the $E1$ transition yields a dominant contribution in the entire energy range up to 1.0 MeV. The contributions of $E2$ and $M1$ transitions are much more suppressed. Even the contribution of the $E2$ transition is less than the contribution from the $E1$ transition by three orders of magnitude at low energy region close to 0 and by two orders of magnitude around the energy value $E = 1$ MeV.

A comparison of the theoretical astrophysical S factor of the radiative direct capture ^{6}Li$(p,\gamma)^7$Be reaction with the experimental data sets from Refs. [21,23,25,49] is shown in Fig. 7. As can be seen from Fig. 7, the calculated astrophysical S factor with the V_M potential model is in good agreement with the direct experimental data of the LUNA Collaboration [25] at low energies. It also gives an overall good description of other experimental data sets in the energy range below 1.0 MeV except for the data set from Ref. [23].

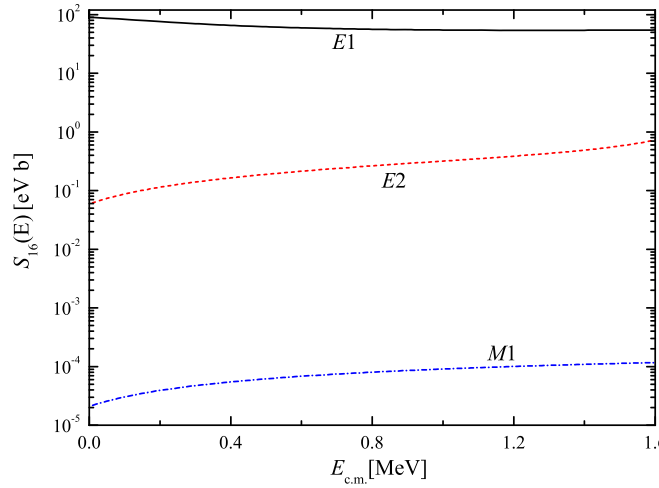

FIG. 6. Contributions of $E1$, $E2$, and $M1$ transition operators to the astrophysical S factor of the ^{6}Li$(p,\gamma)^7$Be synthesis process, calculated within the potential model V_M.

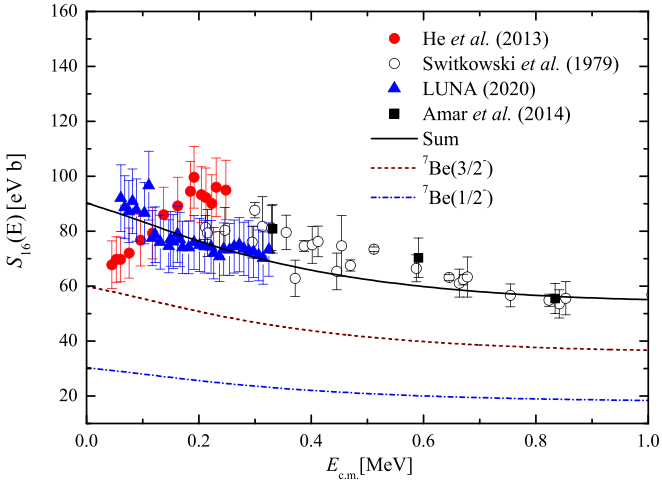

FIG. 7. Astrophysical S factor of the radiative direct capture ^{6}Li$(p,\gamma)^7$Be reaction, calculated with the potential V_M in comparison with the experimental data from Refs. [21,23,25,49].

In Table II we give the calculated values of the astrophysical S factor of the direct ^{6}Li$(p,\gamma)^7$Be capture reaction separately for the ground ^{7}Be$(3/2^-)$ and first excited ^{7}Be$(1/2^-)$ bound states and their sum, at several energies, including the zero and Gamow energy of $E = 15.1$ keV. The zero-energy astrophysical S factor was determined by using the asymptotic expansion method of Ref. [42].

B. Reaction rates of ^{6}Li$(p,\gamma)^7$Be process and primordial abundance of the ^{7}Li element

In nuclear astrophysics, among the most important input quantities for the estimation of primordial abundances of chemical elements in the big bang model of the Universe are the rates of the basis nuclear reactions. The reaction rate $N_A\langle\sigma v\rangle$ is calculated on the basis of calculated cross-section of the process with the help of the following expression [22,50]:

$$N_A\langle\sigma v\rangle = N_A\frac{(8/\pi)^{1/2}}{\mu^{1/2}(k_BT)^{3/2}}\int_0^\infty \sigma(E)E\exp(-E/k_BT)dE, \tag{11}$$

where k_B is the Boltzmann coefficient, T is the temperature, $N_A = 6.0221\times10^{23}$ mol^{-1} is the Avogadro number. The reduced mass μ is determined from the reduced mass number $A = A_1A_2/(A_1+A_2)$ for the $p+^6$Li system. When a variable k_BT is expressed in units of MeV it is convenient to use a variable T_9 for the temperature in units of 10^9 K according to the equation $k_BT = T_9/11.605$ MeV. In present calculations T_9 varies within the interval $0.001 \leqslant T_9 \leqslant 10$.

In these new variables the above integral for the reaction rates can be expressed as

$$N_A\langle\sigma v\rangle = 3.7313\times10^{10}A^{-1/2}T_9^{-3/2} \times\int_0^\infty \sigma(E)E\exp(-11.605E/T_9)dE. \tag{12}$$

The numerical values of the theoretically estimated reaction rates for the ^{6}Li$(p,\gamma)^7$Be direct capture process are given in Table III. A comparison of the calculated reaction rates with the direct experimental data of the LUNA Collaboration [25] and the results of the NACRE II compilation [26], normalized to the NACRE rate [22], are presented in Fig. 8 in the temperature range from $T_9 = 0.001$ to $T_9 = 1$. As can be seen from the figure, the theoretical reaction rates obtained in present work are in good agreement with the direct data of the LUNA Collaboration.

TABLE II. The calculated values of astrophysical S factors for the ground ^{7}Be$(3/2^-)$ and first excited ^{7}Be$(1/2^-)$ ($E^* = 0.429$ MeV) bound states and their sum at energies $E = 0$, 15.1, and 25 keV.

E^* (MeV)	$S(0)$ (eV b)	S(15.1 keV) (eV b)	S(25 keV) (eV b)
0.0	60.0	59.32	48.67
0.429	30.31	29.97	24.54
Total	90.31	89.29	73.21

TABLE III. Theoretical estimates of the direct ^{6}Li$(p,\gamma)^7$Be capture reaction rate $N_A\langle\sigma v\rangle$ (cm^{3}mol^{-1}s^{-1}) in the temperature interval $10^6 \leqslant T \leqslant 10^{10}$ K ($0.001 \leqslant T_9 \leqslant 10$).

T_9	V_M	T_9	V_M
0.001	3.10×10^{-29}	0.14	3.53×10^{-1}
0.002	6.75×10^{-22}	0.15	4.86×10^{-1}
0.003	2.39×10^{-18}	0.16	6.51×10^{-1}
0.004	4.09×10^{-16}	0.18	1.09×10^{0}
0.005	1.57×10^{-14}	0.20	1.69×10^{0}
0.006	2.53×10^{-13}	0.25	4.02×10^{0}
0.007	2.32×10^{-12}	0.30	7.74×10^{0}
0.008	1.44×10^{-11}	0.35	1.30×10^{1}
0.009	6.73×10^{-11}	0.40	1.97×10^{1}
0.010	2.53×10^{-10}	0.45	2.80×10^{1}
0.011	8.06×10^{-10}	0.5	3.77×10^{1}
0.012	2.24×10^{-9}	0.6	6.13×10^{1}
0.013	5.60×10^{-9}	0.7	8.95×10^{1}
0.014	1.27×10^{-8}	0.8	1.22×10^{2}
0.015	2.69×10^{-8}	0.9	1.57×10^{2}
0.016	5.33×10^{-8}	1	1.95×10^{2}
0.018	1.78×10^{-7}	1.25	2.99×10^{2}
0.020	5.02×10^{-7}	1.5	4.10×10^{2}
0.025	3.99×10^{-6}	1.75	5.23×10^{2}
0.030	1.92×10^{-5}	2	6.38×10^{2}
0.040	1.88×10^{-4}	2.5	8.65×10^{2}
0.050	9.44×10^{-4}	3	1.09×10^{3}
0.060	3.20×10^{-3}	3.5	1.30×10^{3}
0.070	8.46×10^{-3}	4	1.51×10^{3}
0.080	1.88×10^{-2}	5	1.90×10^{3}
0.090	3.67×10^{-2}	6	2.26×10^{3}
0.10	6.53×10^{-2}	7	2.60×10^{3}
0.11	1.08×10^{-1}	8	2.92×10^{3}
0.12	1.67×10^{-1}	9	3.23×10^{3}
0.13	2.48×10^{-1}	10	3.51×10^{3}

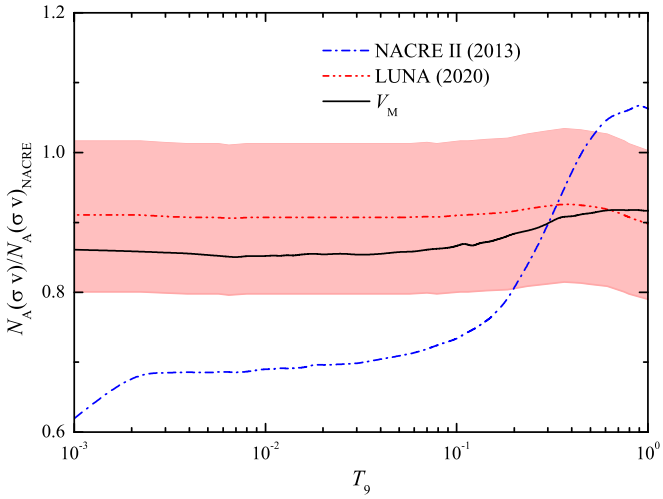

FIG. 8. Comparison of the calculated reaction rates in present potential model for the direct ^{6}Li$(p,\gamma)^7$Be capture process with the results of Refs. [25,26], normalized to the NACRE rate. The shaded area presents the error bar of the LUNA data [22].

In other words, the present theoretical model reproduces not only the absolute values of the reaction rates of the direct experimental data of the LUNA Collaboration, but also the temperature dependence of the reaction rates. As was noted in the Introduction, this point is the most important result of the model, since it does not use any additional parameters for reproducing the LUNA data for the reaction rates. Of course, a success of the theoretical model is connected with a realistic description of the $p+{}^6$Li interaction in important scattering and bound-state channels.

On the other hand, the reproduction of the absolute values of the experimental data for the astrophysical S factor does not give a guarantee that the theoretical reaction rate reproduces the empirical reaction rate and its temperature dependence. This is due to the fact that the astrophysical S factor of the LUNA Collaboration was measured within some error bar, which changes with the energy. Additionally, the reaction rate also was extracted with some error, which depends on the temperature. Indeed, from Fig. 8 one can find that the theoretical reaction rate is almost parallel to the experimental line and the boundaries of the shaded area up to $T_9 = 0.1$, which means that their behavior is almost the same.

As mentioned above, for the estimation of the primordial abundance of the ^{7}Li element the theoretical reaction rate needs to be approximated with the help of an analytical polynomial expression. In our case the numerical results of reaction rate in Table III are reproduced within 0.86 percent by using the following analytical formula:

$$N_{16}(\sigma v) = p_0 T_9^{-2/3}\exp\left(-8.413T_9^{-1/3}\right) \times\left(1+p_1T_9^{1/3}+p_2T_9^{2/3}+p_3T_9+p_4T_9^{4/3}\right) + p_5T_9^{-3/2}\exp\left(-5.634T_9^{-1}\right), \quad (13)$$

The coefficients of the analytical approximation are given in Table IV.

TABLE IV. Fitted values of the coefficients of analytical approximation for the direct capture reaction ^{6}Li$(p,\gamma)^7$Be.

Model	p_0	p_1	p_2	p_3	p_4	p_5
V_M	1.032×10^6	0.369	−0.929	0.492	−0.075	8.197

On the basis of the theoretical reaction rates and with the help of the updated PARTHENOPE 3.0 code [51] we have estimated a contribution from the ^{6}Li$(p,\gamma)^7$Be direct capture reaction to the primordial abundance of the ^{7}Li element. If we use the Planck 2018 data for the baryon density parameter $\Omega_b h^2 = 0.02240 \pm 0.00010$ (or $\eta_{10} = 6.1322 \pm 0.0274$) [52] and the new precision neutron lifetime $\tau_n = 879.4 \pm 0.6$ s from the Particle Data Group [53], for the ^{7}Li/H abundance ratio we have an estimate $(4.67 \pm 0.04)\times10^{-10}$ within the present potential model, which is in good agreement with the BBN result $(4.72 \pm 0.72)\times10^{-10}$ after the Planck observation in Ref. [4].

IV. CONCLUSION

The Astrophysical direct nuclear capture reaction $^6\text{Li}+p\to{}^7\text{Be}+\gamma$ was studied within the two-body single-channel potential model approach. The nuclear $^6\text{Li}-p$ potentials of a Gaussian form with the corresponding Coulomb part have been examined. The parameters of the potential in the partial $^2P_{3/2}$ and $^2P_{1/2}$ waves were fitted to reproduce the binding energies and the empirical values of ANC for the ^{7}Be$(3/2^-)$ ground and ^{7}Be$(1/2^-)$ excited bound states, respectively. The parameters of the potential in the most important $^2S_{1/2}$ scattering wave were fitted to reproduce the empirical phase shifts from the literature and the low-energy astrophysical S factor of the LUNA Collaboration. It is shown that the $E1$ transition from the initial S wave to the final P waves yields a dominant contribution to the astrophysical S factor of the direct capture process. The obtained results for the astrophysical S factor of the ^{6}Li$(p,\gamma)^7$Be reaction are very consistent with the last experimental data of the direct measurement of the LUNA Collaboration and other important experimental data sets from the literature in the energy region up to 1 MeV. The theoretical reaction rates calculated within the model reproduce the both absolute values and temperature dependence of the LUNA data.

The estimated ^{7}Li/H abundance ratio of $(4.67 \pm 0.04)\times10^{-10}$ is in good agreement with the recent BBN ratio of $(4.72 \pm 0.72)\times10^{-10}$ after the Planck observation.

ACKNOWLEDGMENTS

The authors thank L. D. Blokhintsev, D. Baye, and A. S. Kadyrov for useful discussions of the presented results.

[1] M. Lopez-Corredoira, *Fundamental Ideas in Cosmology* (IOP, Bristol, 2022).
[2] E. Grohs and G. M. Fuller, arXiv:2301.12299.
[3] C. E. Rolfs and W. S. Rodney, *Cauldrons in the Cosmos: Nuclear Astrophysics* (University of Chicago Press, Chicago, 1988), p. 338.
[4] B. D. Fields, K. A. Olive, T.-H. Yeh, and C. Young, J. Cosmol. Astropart. Phys. 03 (2020) 010.
[5] D. Clayton, *Handbook of Isotopes in the Cosmos: Hydrogen to Gallium* (Cambridge University Press, Cambridge, 2003).
[6] F. Spite and M. Spite, Astron. Astrophys. **115**, 357 (1982).
[7] A. Gnech and L. E. Marcucci, Nucl. Phys. A **987**, 1 (2019).
[8] D. N. Schramm and R. V. Waronger, Annu. Rev. Nucl. Sci. **27**, 37 (1977).
[9] K. M. Nollett, M. Lemoine, and D. N. Schramm, Phys. Rev. C **56**, 1144 (1997).
[10] M. Anders, D. Trezzi, R. Menegazzo, M. Aliotta, A. Bellini, D. Bemmerer, C. Broggini, A. Caciolli, P. Corvisiero, H. Costantini, T. Davinson, Z. Elekes, M. Erhard, A. Formicola, Z. Fulop, G. Gervino, A. Guglielmetti, C. Gustavino, G. Gyurky, M. Junker, A. Lemut, M. Marta, C. Mazzocchi, P. Prati, C. RossiAlvarez, D.A. Scott, E. Somorjai, O. Straniero, and T. Szucs (LUNA Collaboration), Phys. Rev. Lett. **113**, 042501 (2014).
[11] D. Trezzi, M. Anders, M. Aliotta, A. Bellini, D. Bem-merer, A. Boeltzig, C. Broggini, C. Bruno, A. Caciolli, F. Cavanna *et al.* (LUNA Collaboration), Astropart. Phys. **89**, 57 (2017).
[12] E. M. Tursunov, A. S. Kadyrov, S. A. Turakulov, and I. Bray, Phys. Rev. C **94**, 015801 (2016).
[13] D. Baye and E. M. Tursunov, J. Phys. G: Nucl. Part. Phys. **45**, 085102 (2018).
[14] E. M. Tursunov, S. A. Turakulov, A. S. Kadyrov, and I. Bray, Phys. Rev. C **98**, 055803 (2018).
[15] E. M. Tursunov, S. A. Turakulov, and A. S. Kadyrov, Nucl. Phys. A **1000**, 121884 (2020).
[16] E. M. Tursunov, D. Baye, and S. A. Turakulov, *in Recent Progress in Few-Body Physics*, edited by N. A. Orr *et al.*, (Springer International, Cham, 2020), pp. 119–123.
[17] E. M. Tursunov, S. A. Turakulov, and A. S. Kadyrov, Mem. Soc. astron. ital. **91**, 10 (2020).
[18] E. Vangioni-Flam, M. Casse, and J. Audouze, Phys. Rep. **333-334**, 365 (2000).
[19] A. I. Boothroyd and I.-J. Sackmann, Astrophys. J. **510**, 232 (1999).
[20] H. J. Assenbaum, K. Langanke, and C. Rolfs, Z. Phys. A **327**, 461 (1987).
[21] Z. E. Switkowski, J. C. P. Heggie, D. L. Kennedy, D. G. Sargood, F. C. Barker, and R. H. Spear, Nucl. Phys. A **331**, 50 (1979).
[22] C. Angulo, M. Arnould, M. Rayet, P. Descouvemont, D. Baye, C. Leclercq-Willain, A. Coc, S. Barhoumi, P. Aguer, C. Rolfs (NACRE Collaboration) *et al.*, Nucl. Phys. A **656**, 3 (1999).
[23] J. He, S. Chen, C. Rolfs, S. Xu, J. Hu, X. Ma, M. Wiescher, R. deBoer, T. Kajino, M. Kusakabe *et al.*, Phys. Lett. B **725**, 287 (2013).
[24] T. Szücs, G. G. Kiss, G. Gyürky, Z. Halász, T. N. Szegedi, and Zs. Fülöp, Phys. Rev. C **99**, 055804 (2019).
[25] D. Piatti, T. Chillery, R. Depalo, M. Aliotta, D. Bemmerer, A. Best, A. Boeltzig, C. Broggini, C. G. Bruno, A. Caciolli, F. Cavanna, G. F. Ciani, P. Corvisiero, L. Csedreki, T. Davinson, A. DiLeva, Z. Elekes, F. Ferraro, E. M. Fiore, A. Formicola, Z. Fulop, G. Gervino, A. Gnech, A. Guglielmetti, C. Gustavino, G. Gyurky, G. Imbriani, M. Junker, I. Kochanek, M. Lugaro, L. E. Marcucci, P. Marigo, E. Masha, R. Menegazzo, V. Mossa, F. R. Pantaleo, V. Paticchio, R. Perrino, P. Prati, L. Schiavulli, K. Stockel, O. Straniero, T. Szucs, M. P. Takacs, and S. Zavatarelli (LUNA Collaboration), Phys. Rev. C **102**, 052802(R) (2020).
[26] Y. Xu, K. Takahashi, S. Goriely, M. Arnould, M. Ohta, and H. Utsunomiya (NACRE II Collaboration), Nucl. Phys. A **918**, 61 (2013).
[27] G. X. Dong, N. Michel, K. Fossez, M. Ploszajczak, Y. Jaganathen, and R. M. I. Betan, J. Phys. G: Nucl. Part. Phys. **44**, 045201 (2017).
[28] S. B. Dubovichenko, A. S. Tkachenko, R. Y. Kezerashvili, N. A. Burkova, and A. V. Dzhazairov-Kakhramanov, Phys. Rev. C **105**, 065806 (2022).
[29] K. Arai, D. Baye, and P. Descouvemont, Nucl. Phys. A **699**, 963 (2002).
[30] Z.-H. Li, E.-T. Li, J. Su, Y.-J. Li, Y.-B. Wang, S.-Q. Yan, B. Guo, D. Nan, and W.-P. Liu, Chin. Phys. C **42**, 065001 (2018).
[31] G. G. Kiss, M. LaCognata, R. Yarmukhamedov, K. I. Tursunmakhatov, I. Wiedenhover, L. T. Baby, S. Cherubini, A. Cvetinovic, G. DAgata, P. Figuera, G. L. Guardo, M. Gulino, S. Hayakawa, I. Indelicato, L. Lamia, M. Lattuada, F. Mudo, S. Palmerini, R. G. Pizzone, G. G. Rapisarda, S. Romano, M. L. Sergi, R. Sparta, C. Spitaleri, O. Trippella, A. Tumino, M. Anastasiou, S. A. Kuvin, N. Rijal, B. Schmidt, S. B. Igamov, S.B. Sakuta, Z. Fulop, G. Gyurky, T. Szucs, Z. Halasz, E. Somorjai, Z. Hons, J. Mrazek, R. E. Tribble, and A. M. Mukhamedzhanov, Phys. Rev. C **104**, 015807 (2021).
[32] R. G. Pizzone, R. Sparta, C. A. Bertulani, C. Spitaleri, M. La Cognata, J. Lalmansingh, L. Lamia, A. Mukhamedzhanov, and A. Tumino, Astrophys. J. **786**, 112 (2014).
[33] L. D. Blokhintsev, I. Borbely, and E. I. Dolinskii, Fiz. Elem. Chastits At. Yadra **8**, 1189 (1977) [Sov. J. Part. Nucl. **8**, 485 (1977)].
[34] L. D. Blokhintsev, A. M. Mukhamedzhanov, and A. N. Safronov, Fiz. Elem. Chastits At. Yadra **15**, 1296 (1984) [Sov. J. Part. Nucl. Phys. **15**, 580 (1984)].
[35] A. M. Mukhamedzhanov and N. K. Timofeyuk, Pis'ma Eksp. Teor. Fiz. **51**, 247 (1990) [JETP Lett. **51**, 282 (1990)].
[36] A. M. Mukhamedzhanov and N. K. Timofeyuk, Sov. J. Nucl. Phys. **51**, 431 (1990) [Yad. Fiz. **51**, 679 (1990)].
[37] A. M. Mukhamedzhanov and L. D. Blokhintsev, Eur. Phys. J. A **58**, 29 (2022)
[38] S. B. Dubovichenko, N. Burtebaev, D. M. Zazulin, Z. K. Kerimkulov, and A. S. A. Amar, Phys. At. Nucl. **74**, 984 (2011).
[39] V. T. Voronchev, V. M. Krasnopol'sky, and V. I. Kukulin, J. Phys. G: Nucl. Phys. **8**, 649 (1982).
[40] D. Baye, S. Sauwens, P. Descouvemont, and S. Keller, Nucl. Phys. A **529**, 467 (1991).
[41] D. Baye, P. Descouvemont, and M. Kruglanski, Nucl. Phys. A **550**, 250 (1992).
[42] D. Baye and E. Brainis, Phys. Rev. C **61**, 025801 (2000).
[43] E. M. Tursunov, S. A. Turakulov, and A. S. Kadyrov, Phys. Rev. C **97**, 035802 (2018).
[44] E. M. Tursunov, S. A. Turakulov, and A. S. Kadyrov, Nucl. Phys. A **1006**, 122108 (2021).
[45] E. M. Tursunov, S. A. Turakulov, A. S. Kadyrov, and L. D. Blokhintsev, Phys. Rev. C **104**, 045806 (2021).
[46] A. M. Mukhamedzhanov, Shubhchintak, and C. A. Bertulani, Phys. Rev. C **93**, 045805 (2016).

[47] W. A. Fowler, G. R. Gaughlan, and B. A. Zimmerman, Annu. Rev. Astron. Astrophys. **13**, 69 (1975).
[48] D. Baye, Phys. Rev. Lett. **58**, 2738 (1987).
[49] A. Amar and N. Burtebayev, J. Nucl. Sci. **1**, 15 (2014).
[50] W. A. Fowler, Rev. Mod. Phys. **56**, 149 (1984).
[51] S. Gariazzo, P. F. de Salas, O. Pisanti, and R. Consiglio, Comput. Phys. Commun. **271**, 108205 (2022).
[52] N. Aghanim, Y. Akrami, M. Ashdown, J. Aumont, C. Baccigalupi, M. Ballardini, A. J. Banday, R. B. Barreiro, N. Bartolo, S. Basak (Planck Collaboration) *et al.*, Astron. Astrophys. **641**, A6 (2020).
[53] P. A. Zyla, R. M. Barnett, J. Beringer, O. Dahl, D. A. Dwyer, D. E. Groom, C. J. Lin, K. S. Lugovsky, E. Pianori, D. J. Robinson *et al.* (Particle Data Group), Prog. Theor. Exp. Phys. **2020**, 083C01 (2020).